JOC The Journal of Organic Chemistry

Article

pubs.acs.org/joc

Mechanism of the Enantioselective Intramolecular [2 + 2] Photocycloaddition Reaction of Coumarin Catalyzed by a Chiral Lewis Acid: Comparison with Enone Substrates

Hongjuan Wang, Wei-Hai Fang, and Xuebo Chen*

Key Laboratory of Theoretical and Computational Photochemistry of Ministry of Education, Department of Chemistry, Beijing Normal University, Xin-wai-da-jie 19, Beijing 100875, People's Republic of China

Supporting Information

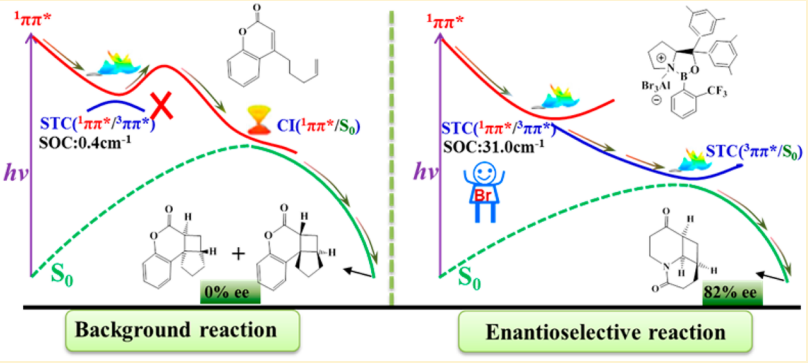

ABSTRACT: The asymmetric catalysis of the intramolecular enone [2 + 2] photocycloaddition reaction relies on a complicated regulation mechanism to control its reactivity and selectivity as well as quantum yield. The multiconfiguration perturbation theory associated with energy-consistent relativistic pseudopotentials offers a mechanistic comparison between representative coumarin and enone substrates. A pair of bright $\pi\pi^*$ states govern the unselective background reaction of the free coumarin through the direct cycloaddition in the singlet hypersurface and the elimination of the reaction channel in the triplet manifold due to the existence of anti El Sayed type singlet−triplet crossing. The opening of a reaction channel in the triplet state is repeatedly verified to depend on the presence of relativistic effects, i.e., spin−orbit coupling due to heavy atoms in the chiral Lewis acid catalyst.

INTRODUCTION

The [2 + 2] cycloaddition (CA) reaction has developed from an academic curiosity to an excellent tool in organic synthesis and has shown interesting reactivity and selectivity, affording regio- and stereoselective synthetic transformations.[1−8] However, the thermal [2 + 2] reaction is forbidden as a supra−supra process by Woodward−Hoffmann rules and requires high temperatures (>200 °C), suffering from generally low yields.[3,9,10] An alternative solution, recognized as early as 1912, indicates that light serves as an environmentally friendly reagent that allows the [2 + 2] CA reaction to proceed in a photocycloaddition (PCA) manner via high energy excited states with a satisfactory yield of cyclobutane product.[11] To expand vibrantly its application to biologically interesting compounds, such as drugs, agrochemicals, food additives, and fragrances, a large variety of methods have been developed for the selective preparation of enantiomerically pure compounds with a high enantiomeric excess (ee).[2,4,5,12−16]

The conventional approach was first adopted by using a chiral auxiliary to which [2 + 2] photocycloaddition substrates bind via covalent interactions, leading to exciplex formation, and which are capable of inducing asymmetry in the subsequent photochemical transformation.[17−19] The chiral auxiliary group is split off and can thus be recovered under mild conditions after the cycloaddition.[17−19] In contrast to the two-step approach, a notable strategy is to employ noncovalent interactions between the catalyst and its substrate to provide a chiral environment. By using several entities of this type including cyclodextrins[20−23] and hydrogen-bonding templates,[24−29] the direct approach shows an excellent performance in both enantioselectivity and yield and has the advantage that it is not necessary to first add and then remove the auxiliary.

As a promising solution, the Lewis acid catalysts have been considered as potential chiral templates to carry out enantioselective photochemical reactions. This idea was inspired by the experimental discovery of Lewis et al., where the BF_3 or $EtAlCl_2$ can be observed to catalyze the intermolecular [2 + 2] photocycloaddition of coumarin and different olefins.[30,31] Following the previous works regarding

Special Issue: Photocatalysis

Received: April 29, 2016
Published: June 20, 2016

DOI: 10.1021/acs.joc.6b00980
J. Org. Chem. 2016, 81, 7093−7101

Scheme 1. Enantioselective Intramolecular [2 + 2] Photocycloaddition Reaction of Coumarin 2 and Enone Substrate 3 Mediated by Chiral Lewis Acid 1

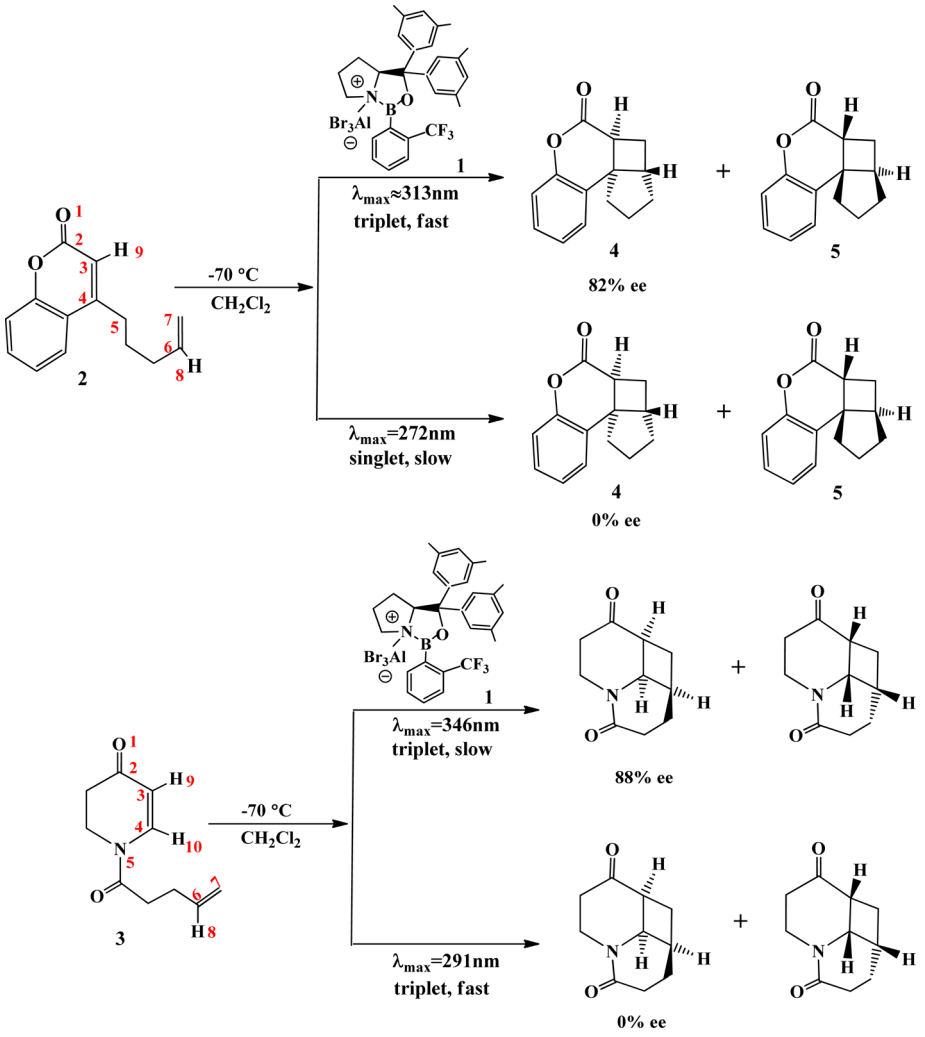

the thermal cycloaddition reactions catalyzed by a chiral Lewis acid,[32−35] Bach and his co-workers applied chiral oxazaborolidine-$AlBr_3$ based Lewis acid catalyst (**1** see Scheme 1) to enable the enantioselective intramolecular [2 + 2] PCA of coumarin (**2**) and a typical enone substrate, i.e., 5,6-dihydro-4-pyridones (**3**).[36−39] As shown in Scheme 1, the stereochemical PCA products **4** and **5** were obtained with satisfactory yield (~0.84) and high enantioselectivity (82−90% ee) in the presence of catalyst **1** when the unselective background reaction was noticeably suppressed at high catalyst loadings (typically ~50 mol %). However, the mechanistic courses of coumarins were found to be totally different from the PCA reaction of dihydropyridones. For the former ones, the reaction takes place in the singlet pathway whereas the dihydropyridones underwent a fast triplet reaction in the absence of the Lewis acid.[36,39] In contrast, the triplet manifold becomes the predominant precursor for the Lewis acid catalyzed reactions of coumarins and dihydropyridones.[36,39] In comparison with the uncatalyzed background reactions, the reaction rates were accelerated for the cycloaddition reaction of coumarins but slowed down in the presence of a chiral Lewis acid of dihydropyridones.[36,39]

All these experimental observations indicate that it is a challenging issue to understand the regulatory mechanism mediated by the chiral Lewis acid and to effectively suppress the unselective background reaction. To achieve a general strategy for controlling racemic background reactions, an innovative approach was developed in Yoon's group[7,40−46] by the introduction of one more transition-metal complex that is able to trigger the photoredox reaction regulated by single-electron transfer.[47−50] Although substantial progress has been achieved in past decades, the mechanistic understanding of the effect of the Lewis acid and the photocatalyst of transition metal on the reaction course seriously lags behind the wealth of experimental investigations.[16] It is desirable to perform state-of-the-art theoretical studies. In a successful attempt, the mechanism of the catalyzed and unselective background reactions for a typical enone substrate **3** has been rationalized theoretically in our group.[51] We proposed a regulatory mechanism in which the enantioselective reaction is predominantly controlled through the alternation of energy levels $n\pi^*/\pi\pi^*$ in the presence of relativistic effects, that is, spin−orbit coupling resulting from the heavy atoms of chiral Lewis acid. In this work, we therefore employed the same multiconfigurational quantum chemical approach associated with relativistic energy-adjusted ab initio pseudopotentials[52,53] that has been verified to be superior in investigations of excited states of various systems containing heavy atoms with comprehensive consideration of

DOI: 10.1021/acs.joc.6b00980
J. Org. Chem. 2016, 81, 7093−7101

Table 1. Vertical Excitation Energies ($E_\perp$, kcal/mol), Oscillator Strengths (f), Transition Dipole Moments (ΔDM, Debye), Spin-Orbit Coupling (SOC, cm^{-1}) between the S_{PP} ($^1\pi\pi^*$) and T_{CT}($^3\pi\pi^*$) States, as Well as the Character of Singly Occupied Orbitals for the $S_0 \rightarrow S_{PP}(^1\pi\pi^*)$, $S_0 \rightarrow S_{CT}(^1\pi\pi^*)$, and $S_0 \rightarrow S_{NP}(^1n\pi^*)$ Electronic Transitions of 2, 2−BF_3, and 2−1[a]

	Transitions	$E_\perp$	f	ΔD.M.	SOC S_{PP}/T_{CT}	Singly occupied orbitals
2	$S_0 \rightarrow S_{PP}(^1\pi\pi^*)$	96.7 (91.3)	0.16	4.87→4.53		$\pi_1 \rightarrow \pi^*$
	$S_0 \rightarrow S_{CT}(^1\pi\pi^*)$	109.8 (105.1)	0.30	4.87→7.65	0.4	$\pi_2 \rightarrow \pi^*$
	$S_0 \rightarrow S_{NP}(^1n\pi^*)$	112.2	8.13E-04	4.87→1.42		$n \rightarrow \pi^*$
2-BF_3	$S_0 \rightarrow S_{PP}(^1\pi\pi^*)$	96.1 (91.3)	0.32	9.59→14.10		$\pi_1 \rightarrow \pi^*$
	$S_0 \rightarrow S_{CT}(^1\pi\pi^*)$	100.8	0.54	9.59→15.56	0.8	$\pi_2 \rightarrow \pi^*$
	$S_0 \rightarrow S_{NP}(^1n\pi^*)$	138.6	5.34E-04	9.59→3.51		$n \rightarrow \pi^*$
2-1	$S_0 \rightarrow S_{PP}(^1\pi\pi^*)$	93.4 (89.3)	0.50	13.9→11.47		$\pi_1 \rightarrow \pi^*$
	$S_0 \rightarrow S_{CT}(^1\pi\pi^*)$	100.7	0.40	13.9→13.46	31.0	$\pi_2 \rightarrow \pi^*$
	$S_0 \rightarrow S_{NP}(^1n\pi^*)$	126.6	5.28E-04	13.9→12.80		$n \rightarrow \pi^*$

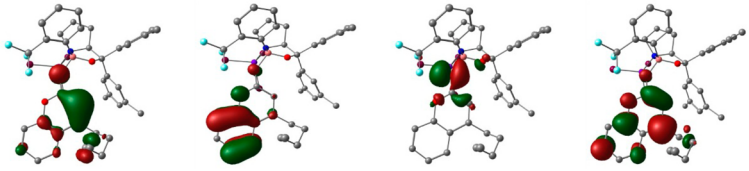

π_1 π_2 n π^*

[a]The experimental values (ref 39) are shown in parentheses for comparison. The schematic orbitals of **2−1** are given as an example.

dynamic electron correlation and relativistic effects. The purpose of the present study is to investigate **2** and its coordinated complexes with different Lewis acid catalysts and to disclose the similarities and differences of the two substrate classes **2** and **3** in an enantioselective intramolecular [2 + 2] PCA reaction.

■ COMPUTATIONAL DETAILS

The complete active space self-consistent field (CASSCF) method with the aid of the second-order perturbation theory based on the CASSCF reference (CASPT2) has a certain superiority in computing several states of a system and makes it possible to easily distinguish between different electronic transitions. Comprehensively considering the electron correlation effect, the CASPT2//CASSCF approach can accurately describe the electronic spectra and properties of the excited state, especially for those excited states with charge-transfer (CT) character[54,55] and strong spin−orbit coupling effects.[56,57] In this work, the ab initio calculations of isolated coumarin **2** were primarily performed at the CASSCF level with a total of 10 electrons in nine orbitals (10e/9o) and 6-31G* basis sets, and this level of theory is referred to as CASSCF(10e/9o)/6-31G*. To describe the reaction processes of [2 + 2] PCA, π orbitals and their corresponding π^* orbitals of C3═C4 and C6═C7 (see Scheme 1 for atom numbering) were included in the active space. Meanwhile, the O1 lone pair and two π/π^* pairs of aromatic rings were added into the active space to account for the possible regulatory role of the $n\pi^*$ state and $\pi \rightarrow \pi^*$ electron transitions, respectively.

To describe the coordination effect between the substrate and the Lewis acids, the coordinated empty 2p orbital of the B atom was also added into the active space in addition to the included n orbital of the carbonyl oxygen O1 for substrate **2**. To better account for the possible relativistic effects from Br or F, the corresponding lone pair of Br or F was also added into the active space, thus resulting in a total 12e/10o active space for the **2**−oxazaborolidine−$AlBr_3$ (**2−1**) and **2**−BF_3 complexes. The CASSCF reference wave function was initially generated from the Hartree−Fock natural orbitals. All these orbitals in the active space for the free **2**, **2−1**, and **2**−BF_3 complexes are schematically shown in Figures S1−S3 of the Supporting Information (SI). For the **2**−BF_3 complex, the 6-31G* basis set was applied for all atoms.

Huge computational resources are required to perform CASPT2//CASSCF(12e/10o) computations for the **2−1** complex with 97 atoms since the approach shows an exponential increase in the demand for computational resources with system size. Therefore, the basis set must be reduced to balance the accepted calculation errors and the available computational resources. An energy-consistent scalar-relativistic WB-adjusted 28-electron core pseudopotential[52,53] was chosen to describe the relativistic effects involved in the calculations of heavy bromine atoms. Meanwhile, the corresponding ECP28MWB_VTZ ((14s10p2d1f)/ [3s3p2d1f]) basis set for the Br atoms was applied in the optimizations of all critical points and the corresponding intrinsic reaction coordinate (IRC)[58,59] computations at the CASSCF level of theory. All other lighter atoms were treated at the all-electron level. The 6-31G* basis set was applied for the atoms at the reacting center, i.e., coumarin **2** and its coordinated pyrrole ring of oxazaborolidine, as well as the Al and F atoms, while the STO-3G basis set was adopted for the rest of the atoms. To avoid a memory disaster for such a large system using the high level of CASPT2//CASSCF(12e/10o) calculations, the basis sets of ECP28MWB_VTZ and 6-31G* were replaced by the smaller ECP28MWB ((6s6p1d)/ [5s5p1d]) and 6-31G sets in the single-point energy calculations at the CASPT2 level of theory, based on optimized geometries using the CASSCF method with the aforementioned large basis sets. The calculated excitation and emission energies were found to be in good agreement with available experimental spectral data.[39] All of the parameters for pseudopotentials and valence basis sets of the Br atoms were taken from the homepage of the Dolg group (http://www.tc.uni-koeln.de/PP/index.en.html) and the basis set library of the Molcas program package.[60]

All of the minima in the singlet excited state were obtained by full system state-averaged CASSCF optimizations using a two-root equally weighted (0.5:0.5) approach, whereas a single root optimization was adopted in the triplet and ground states. The same state-averaged method was employed to determine the geometry of the intersection space of the two electronic states with the same spin multiplicity, and

DOI: 10.1021/acs.joc.6b00980
J. Org. Chem. 2016, 81, 7093−7101

the minimum energy crossing points between the singlet and triplet states were optimized using Slater determinants.[61] All of the optimized critical structures for **2**, **2**−BF_3, and **2**−**1** have been schematically summarized in section 3 of the SI. For isolated **2** and the **2**−BF_3 complex, the transition state (TS) optimization and frequency analyses for selective saddle points and minimum points were carried out at the CASSCF level of theory with a reduced active space of 10e/8o by excluding the high-lying π^* orbital for **2** and its corresponding π orbital for **2**−BF_3. For the **2**−**1** complex, the TS optimization and frequency analyses in triplet state have been primarily done at the density functional theory (DFT) level using the B3LYP functional with the same basis set strategy as the CASSCF computations. By using starting geometries optimized at the DFT level, the TS structure was reoptimized at the CASSCF level of theory, which was followed by IRC computations. The minimum energy profiles (MEPs) were mapped by IRC computations to connect above critical points in several possible excited and ground states. To consider dynamic electron correlation effects, the single-point energy of the optimized geometries in the above computations was recalculated at the multiconfiguration second-order perturbation level of theory[62,63] based on the zeroth-order five root state-averaged CASSCF wave functions with the equal weights. Therefore, the MEPs were eventually computed at the CASPT2//IRC/CASSCF (12e/10o) level of theory along the unbiased reaction coordinates to gain insight into how the Lewis acid catalyzed intramolecular [2 + 2] cycloaddition reaction takes place. The vertical excitation energies and the corresponding oscillator strengths (f) for the different transitions of **2**, **2**−BF_3, and **2**−**1** were calculated by five root state-averaged CASSCF state interaction (CASSI) computations based on the geometries of the S_0 minimum. The spin−orbit coupling (SOC) between the singlet and triplet states was also computed using the CASSI approach with effective spin−orbit terms for F and Br atoms. In this work, all of the DFT and CASSCF calculations, together with the IRC pathway calculations, were performed using the Gaussian program package,[64] whereas the CASPT2 computations were carried out with the Molcas program package.[60]

RESULTS AND DISCUSSION

Vertical Excitation of 2, 2−BF_3, and 2−1. Table 1 summarizes the vertical excitation energies ($E_\perp$, kcal/mol), oscillator strengths (f), and changes of dipole moment (ΔDM, debye) of different transitions for **2** and its complexes (**2**−BF_3 and **2**−**1**) as well as the assignment of the excited-state character. A pair of bright spectroscopic states were found for the free coumarin with a similar magnitude of the oscillator strength (0.16 and 0.30) that are 200−400-fold larger than that of the n → π^* transition. The electronic population of absorption maximum (latter one) indicates that the unpaired electrons are distributed in the phenyl ring and C3═C4 double bond of the enone moiety, respectively. This result indicates that this strongest absorption (f = 0.30) exhibits a significant CT character and therefore is referred as the $S_0 \rightarrow S_{CT}(^1\pi\pi^*)$ transition. According to the population analyses and charge translocation calculations (see section S2 in the SI), a large, photoinitiated charge translocation (PICT) with 0.31 e was found from the phenyl ring to the C3═C4 double bond. Consistently, the calculated dipole moment increases from S_0 (4.87 D) to $S_{CT}(^1\pi\pi^*)$ (7.65 D) upon Franck−Condon (FC) excitation. The calculated vertical excitation energy ($E_\perp$), 109.8 kcal/mol (260 nm), is close to that of the experimental maximum absorption wavelength, $\lambda_{max,abs}$ (272 nm), with the largest extinction coefficients (ε = 11100 M^{-1} cm^{-1}).[39]

Unlike $S_0 \rightarrow S_{CT}(^1\pi\pi^*)$ excitation with an obvious CT character, another bright spectroscopic state initially originates from the local $\pi \rightarrow \pi^*$ transition of C3═C4 double bond, denoted as $S_{PP}(^1\pi\pi^*)$ (see Table 1). It should be pointed out that the conjugate effect between the C3═C4 double bond and the phenyl ring as well as the O1═C2 carbonyl group causes this local excitation to mix with a slight CT character. This may explain why the local $S_0 \rightarrow S_{PP}(^1\pi\pi^*)$ excitation for the isolated coumarin has modest oscillator strength (f = 0.16) and shows a slight change in dipole moment. The calculated vertical excitation energy is 96.7 kcal/mol (ca. 296 nm), which is 17 nm blue-shifted with the experimentally observed long wavelength region at 313 nm (ε = 6400 M^{-1} cm^{-1}).[39]

Similar to the case of enone substrate **3**, the dark spectroscopic $S_{NP}(^1n\pi^*)$ state for the free **2** that originates from the promotion of one electron of the O1 lone pair to a π^* orbital of the whole conjugated ring in both enone part and the distal phenyl ring was also determined. This alters the traditional diradical configuration of n → π^* excitation with the mixture CT character to some extent. However, for the enone substrate **3**, the corresponding π^* of the n → π^* excitation is the localized π^* orbital of the C3═C4 double bond, leading to a traditional diradical configuration without any CT mixture. Consistently, the vertical excitation energy of $S_0 \rightarrow S_{NP}(^1n\pi^*)$ for coumarin is ca. 27.4 and 2.4 kcal/mol higher than that of enone substrate **3** and $S_{CT}(^1\pi\pi^*)$ of the free **2**, respectively, due to the electron promotion of the oxygen lone pair over a long distance. Meanwhile, the dipole moment shows a noticeable decrease from S_0 (4.87 D) to $S_{NP}(^1n\pi^*)$ (1.42 D). This improved energy level eliminates the possible role of the $S_{NP}(^1n\pi^*)$ state in the mechanistic regulation of the initial population and subsequent PCA reaction for the free coumarin **2**, whereas the racemic background reaction of the free enone substrate **3** was found to be controlled by the nπ^* intermediate state.

The energetic level of the $S_{NP}(^1n\pi^*)$ state continuously rises up to 138.6/126.6 kcal/mol with respect to the zero level of S_0 minima for **2**−BF_3 and **2**−**1** upon Lewis acid coordination (see Table 1). This is due to an electron-withdrawing effect imposed by the electron deficiency of boron on the carbonyl moiety C2═O1, thus blocking the electron promotion of the O1 lone pair. As a result, the $S_{NP}(^1n\pi^*)$ state completely loses the opportunity to regulate the catalyzed PCA reaction mediated by chiral or nonchiral Lewis acids. On the other hand, the coordination of B−O facilitates the charge transfer from the phenyl ring to the C3═C4 double bond, therefor lowering the energetic level of the $S_{CT}(^1\pi\pi^*)$ state (ca.100 kcal/mol) of **2**−BF_3 and **2**−**1**. However, this enhanced charge transfer exerts a negligible perturbation on the local $S_0 \rightarrow S_{PP}(^1\pi\pi^*)$ excitation, which reduces the energy gap between the $S_{CT}(^1\pi\pi^*)$ and $S_{PP}(^1\pi\pi^*)$ states. As an important consequence, these two excited states become energetically indistinguishable in the FC excitation of **2**−BF_3 and **2**−**1** complexes. The present computational results account for the absorption spectra of coumarin−Lewis acid complexes in which a strong UV−vis absorption at λ = 313 nm was observed experimentally, while the intensity of the short wavelength absorption decreases.[36,39]

Racemic Background Reaction of Free 2. Figure 1 shows MEPs of [2 + 2] PCA for the isolated coumarin. Upon the photoexcitation at 260 nm, the free **2** is instantaneously populated in the FC region of $S_{CT}(^1\pi\pi^*)$ state and then rapidly decays along a downhill path. The remarkable changes in structure are mainly associated with the weakened C3═C4 double bond (1.35 → 1.50 Å) and the concomitant enlarged phenyl ring with elongation of some C−C bonds (1.40 → 1.44−1.48 Å). These structural arrangements confirm the CT nature of the $S_0 \rightarrow S_{CT}(^1\pi\pi^*)$ transition that originates from

DOI: 10.1021/acs.joc.6b00980
J. Org. Chem. 2016, 81, 7093−7101

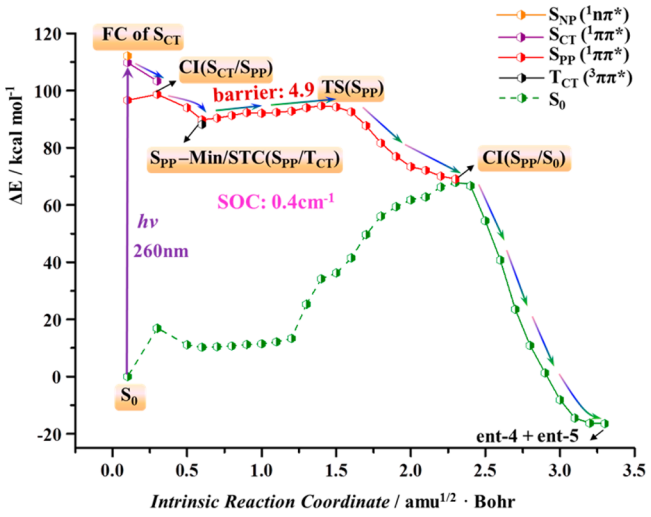

Figure 1. Minimum energy profiles of the [2 + 2] photocycloaddition for the isolated coumarin **2** obtained at the CASPT2//IRC//CASSCF(10e/9o) level of theory. The related [2 + 2] cycloaddition barrier is given in kcal/mol. The structures at the highlighted characteristic points of the reaction path are provided, with their key bond distances, in the SI.

the charge translocation along the desired direction from the phenyl ring to the C3═C4 double bond. The initial relaxation in the $S_{CT}(^1\pi\pi^*)$ state leads to a decrease in energy of 6.0−7.0 kcal/mol, while the energy of $S_{PP}(^1\pi\pi^*)$ state is slightly shifted up due to the enlarged phenyl ring. As a result, these two excited states intersect each other to seam the surface of $S_{CT}(^1\pi\pi^*)$ and $S_{PP}(^1\pi\pi^*)$ states at the conical intersection (CI) region that is denoted as $CI(S_{CT}/S_{PP})$. The $CI(S_{CT}/S_{PP})$ functions as an effective nonadiabatic relay to repopulate the free coumarin in $S_{PP}(^1\pi\pi^*)$ state from the $S_{CT}(^1\pi\pi^*)$ state. The C3−C4 bond undergoes a slight strengthening (ca. 1.48 Å) in the $S_{PP}(^1\pi\pi^*)$ state together with the somewhat shrunken phenyl ring along a downhill path. These structural changes reflect the character of local excitation with a slight mixture of CT character for the $S_0 \rightarrow S_{PP}(^1\pi\pi^*)$ transition.

Unlike the decay in the bright $^1\pi\pi^*$ state for the enone substrate **3**, the structural deformation of C3−H9 twisting of free coumarin was not triggered in the relaxation of $S_{CT}(^1\pi\pi^*)$ and Spp($^1\pi\pi^*$) states. This is largely due to the structural constraint in the presence of rigid aromatic ring. As a consequence, the reaction channel of PCA for the free coumarin in the ground state is completely closed due to the absence of conical intersection caused by the structural twisting between the bright $^1\pi\pi^*$ and the ground states. Thus, there are two possible decay channels starting from the minimum of $S_{PP}(^1\pi\pi^*)$ state, i.e., the direct PCA reaction in $S_{PP}(^1\pi\pi^*)$ state and intersystem crossing (ISC) to the triplet state. The energy gaps between the $S_{PP}(^1\pi\pi^*)$ state and the $T_{PP}(^3\pi\pi^*)$ as well as $T_{CT}(^3\pi\pi^*)$ states were examined rigorously along the MEP of $S_{PP}(^1\pi\pi^*)$ state. The minimum difference between $S_{PP}(^1\pi\pi^*)$ and $T_{CT}(^3\pi\pi^*)$ states is 1.5 kcal/mol when the free coumarin approaches the S_{PP}-Min. This indicates that there exists the singlet triplet crossing (STC) between the $^1\pi\pi^*$ and $^3\pi\pi^*$ states from the viewpoint of energy degeneracy. However, the spin−orbit coupling (SOC) is calculated to be only 0.4 cm^{-1}, suggesting an ineffective ISC of $^1\pi\pi^* \rightarrow {}^3\pi\pi^*$ through an anti El Sayed type crossing.[65−68] Therefore, the triplet manifold for the free coumarin unlikely functions as an effective precursor state for the subsequent PCA reaction due to a very small possibility of triplet access. This totally changes the case of enone substrate **3** where $^1n\pi^*$ state serves as an effective intermediate leading to a fast ISC of $^1n\pi^* \rightarrow {}^3\pi\pi^*$ via an El Sayed type crossing.[65−68]

On the contrary, the direct PCA reaction in the $S_{PP}(^1\pi\pi^*)$ state proceeds smoothly along a relatively flat path. Starting from $CI(S_{CT}/S_{PP})$, the initial geometric arrangement is characterized by the torsional deformation of the distal C6═C7 double bond, leading to a face-to-face architecture with respect to the C3−C4 bond. Meanwhile, the energy of $S_{PP}(^1\pi\pi^*)$ goes down slightly with the concomitant shortening of C3−C7 distance (4.57 → 3.72 Å), which prepares for the subsequent PCA reaction. In the following C6═C7 bond

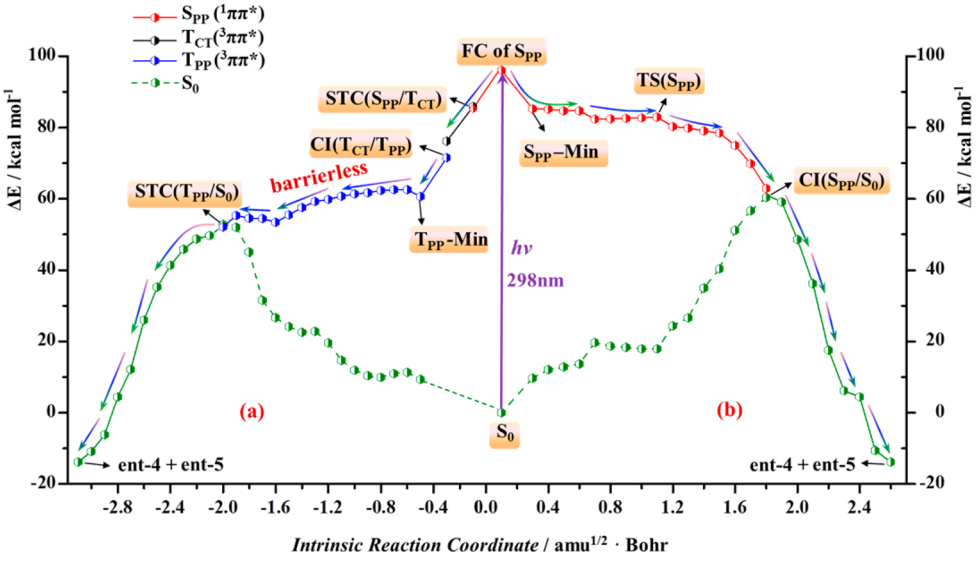

Figure 2. Minimum energy profiles of the [2 + 2] photocycloaddition for the **2**−BF_3 complex on the triplet (a) and singlet (b) states obtained at the CASPT2//IRC//CASSCF(12e/10o) level of theory. The structures at the highlighted characteristic points of the reaction path are given with their key bond distances in the SI.

DOI: 10.1021/acs.joc.6b00980
J. Org. Chem. 2016, 81, 7093−7101

approach, C6 goes slower than C7 to wait for the arrival of C7. The C3−C7 distance (2.61 Å) is very close to that of C4−C6 (2.48 Å) when the free coumarin surmounts the transition state of PCA, TS(S_{PP}), by overcoming a small barrier (ca. 4.9 kcal/mol) at the singlet $^1\pi\pi^*$ hypersurface. This structural characteristic of TS(S_{PP}) give a hint that cycloaddition could proceed in a concerted manner. Further evidence comes from the geometric resemblance in the conical intersection between the $S_{PP}(^1\pi\pi^*)$ and ground states, CI(S_{PP}/S_0), whose energy is 25.6 kcal/mol below that of TS(S_{PP}). The C3−C7 and C4−C6 distances are simultaneously shortened to ∼2.20 Å in CI(S_{PP}/S_0) while the C6−C7 bond is elongated to be 1.43 Å from 1.34 Å in S_{PP}-Min, and this value is very close to that of C3−C4 bond (1.46 Å) in CI(S_{PP}/S_0).

Unlike the case of the aforementioned STC($^1\pi\pi^*/^3\pi\pi^*$), the energy degeneracy between $S_{PP}(^1\pi\pi^*)$ and S_0 states with the same multiplicity enables an effective internal conversion to the ground surface. Once the free **2** is populated in the ground state, C6 and C7 simultaneously attack C4 and C3 from two different directions of the conjugate ring to achieve the concerted cycloaddition reactions producing **4** and its enantiomer **5**. Therefore, the direct PCA reaction in the singlet pathway is the predominant relaxation channel regulated by a pair of bright $^1\pi\pi^*$ states in comparison with an ineffective ISC of $^1\pi\pi^* \rightarrow {}^3\pi\pi^*$ through an anti-El-Sayed-type crossing for the uncatalyzed coumarin reactions, whereas the triplet manifold is the precursor state for the PCA reaction of enone substrate **3** mediated by an energetically accessible $^1n\pi^*$ state via an El Sayed type singlet−triplet crossing.[51]

Enantioselective Reaction Mediated by a Chiral Lewis Acid Catalyst. Upon coordination of coumarin **2** with nonchiral (BF_3) and chiral **1** catalysts, modification of the mechanistic aspect was found to be mainly associated with the opening of the reaction channel in the triplet state as shown in Figures 2 and 3. As discussed above, a pair of bright states, i.e., $S_{CT}(^1\pi\pi^*)$ and $S_{PP}(^1\pi\pi^*)$, energetically get closer in FC excitation of **2**−BF_3 and **2**−**1** complexes. This suggests that the initial population of the $S_{PP}(^1\pi\pi^*)$ state for the coordinated

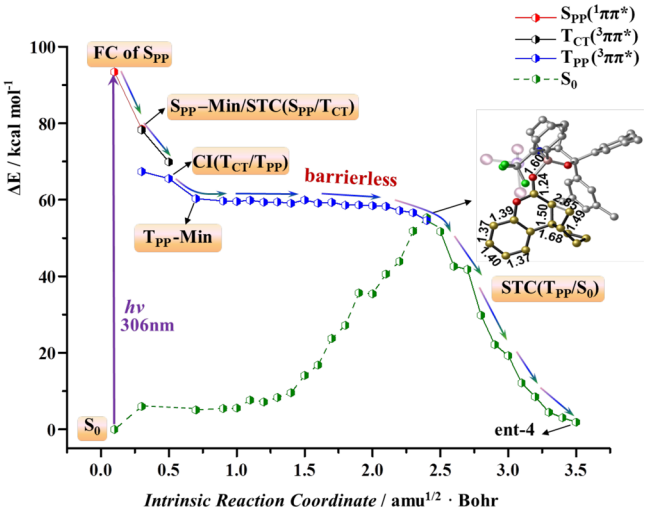

Figure 3. Minimum energy profiles of the [2 + 2] photocycloaddition for the **2**−**1** complex obtained at the CASPT2//IRC//CASSCF(12*e*/10o) level of theory. The structures at the highlighted characteristic points of the reaction path are given with their key bond distances in the SI.

coumarin becomes more efficient through the anticipatory occurrence of internal conversion or the direct excitation in the FC region compared with the case of free **2**. Moreover, the CT character of the $S_{PP}(^1\pi\pi^*)$ state is further enhanced along the desired direction from the C3═C4 moiety to the C2═O1 carbonyl group induced by the electron deficiency of boron and the aid of the electron-donating group of phenyl ring. This leads to the ultrafast relaxation of coumarin−catalyst complexes from the FC of the $S_{PP}(^1\pi\pi^*)$ state to extremely stabilized minima (S_{PP}-Min) in the excited singlet state with a significant decrease in energy (10.8−14.9 kcal/mol). The adiabatic excitation energies of the $S_{PP}(^1\pi\pi^*)$ state were calculated to redshift from 89.8 kcal/mol of the free coumarin **2** to 78.5/85.3 kcal/mol of **2**−**1**/**2**−BF_3 complexes. The stabilization difference is attributed to the structural character of the $S_{PP}(^1\pi\pi^*)$ state in which the minimum of the $S_{PP}(^1\pi\pi^*)$ state for **2**−**1** exhibits a resonance structure of the allylic system (i.e., the shortened C2−C3 bond together with the elongated C3═C4 and O1═C2 bonds) compared with that of **2**−BF_3 as shown in section 3 of the SI.

Similarly, the energetic level of the transition state for the direct PCA reaction in the $S_{PP}(^1\pi\pi^*)$ state, i.e., TS(S_{PP}), goes down to ca. 83.0 kcal/mol for the catalyzed reaction of the **2**−BF_3 complex from 94.7 kcal/mol for the background reaction in the absence of Lewis acid catalyst. As a result, the unselective background reaction in the singlet hypersurface is considerably suppressed by the alternation of the irradiation source from 300 to 366 nm since the direct PCA reaction in the $S_{PP}(^1\pi\pi^*)$ state for the free coumarin **2** is energetically inaccessible under the excitation wavelength λ = 366 nm (78.1 kcal/mol). However, the Lewis acid catalyzed [2 + 2] PCA reaction in the singlet state is still open for the coumarin−catalyst complexes upon high energy excitation.

The energy gap between $S_{PP}(^1\pi\pi^*)$ and $T_{CT}(^3\pi\pi^*)$ is reduced to <1.0 kcal/mol when **2**−**1**/**2**−BF_3 complexes approach S_{PP}-Min, which indicates that there exists a crossing between $S_{PP}(^1\pi\pi^*)$ and $T_{CT}(^3\pi\pi^*)$ states that is referred to as STC(S_{PP}/T_{CT}). Like the case of enone **3**−**1** complex, a large SOC of 31.0 cm^{-1} for **2**−**1** is found over an extended region of STC(S_{PP}/T_{CT}), allowing an effective ISC between the singlet and triplet states with the same nature of the $\pi \rightarrow \pi^*$ transition. In contrast, a much smaller SOC (0.8 cm^{-1}) is determined at the STC(S_{PP}/T_{CT}) of **2**−BF_3 when the coumarin is coordinated with the same boron-based catalyst, but without bromine atoms. The relativistic effects due to the presence of heavy atoms are repeatedly verified to play a decisive role in the improvement of the intersystem-crossing rate and the increase of the PCA yield.[51] Compared with the free coumarin **2**, the SOC of **2**−BF_3 complex increases 1-fold (0.4 → 0.8 cm^{-1}), thus allowing the generation of a partial outcome of the photochemical reaction from the triplet state. Therefore, the coexistence of the reaction channels in both singlet and triplet states is responsible for the nonchiral Lewis acid catalyzed [2 + 2] PCA reaction (**2**−BF_3) in the presence of boron-based catalyst, but without heavy atom (see Figure 2). Once the heavy atom of bromine is introduced to the chrial catalyst (**2**−**1**), the ISC rate is dramatically increased due to the enhanced SOC. As an important result, the more effective PCA reaction characterized with the barrierless path in triplet manifold predominantly controls the Lewis acid catalyzed processes of **2**−**1** to deliver enantioselective product (see Figure 3). Consistently, a much higher yield (97%) was observed experimentally in the $AlBr_3$-catalyzed PCA reaction compared

DOI: 10.1021/acs.joc.6b00980
J. Org. Chem. 2016, 81, 7093−7101

Scheme 2. Plausible Mechanism of the Intramolecular [2 + 2] Photocycloaddition Reaction of Coumarin in the Absence and Presence of the Chiral Lewis Acid

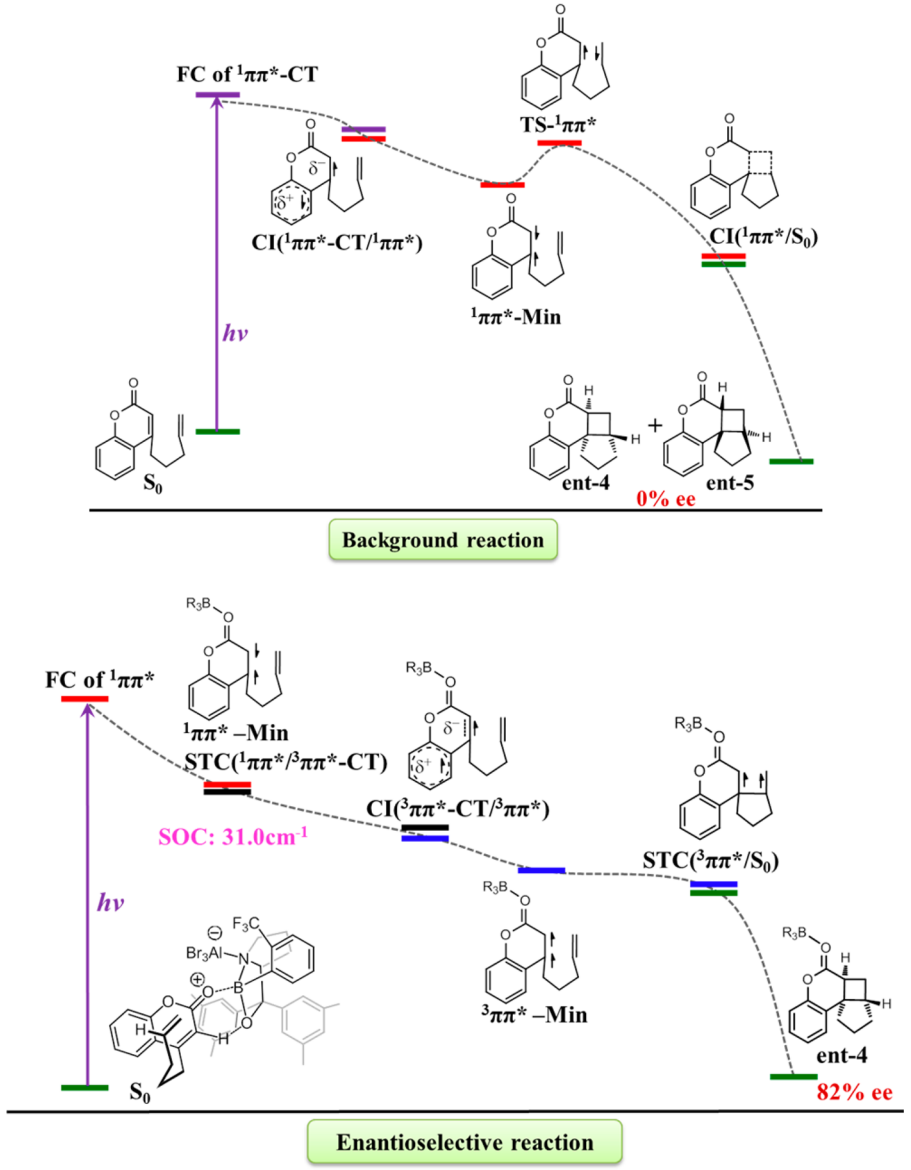

with a yield of 33% when using a $BF_3{\cdot}OEt_2$ catalyst under the same conditions.[37]

Following the highly effective ISC from $S_{PP}(^1\pi\pi^*)$ to $T_{CT}(^3\pi\pi^*)$ states, a conical intersection of $CI(T_{CT}/T_{PP})$ was found to funnel the nonadiabatic conversion of **2**−**1** to its reactive $T_{PP}(^3\pi\pi^*)$ state. Once **2**−**1** was populated in the $T_{PP}(^3\pi\pi^*)$ state, the [2 + 2] PCA reaction was immediately triggered to proceed in a stepwise manner. The torsional deformation of the distal C6═C7 double bond initially led to the shortened C4−C6 and C3−C7 distances. When the C3−C7 distance was shortened to ca. 2.8 Å, a carbon−carbon bond started to form between C4 and C6 atoms along a relatively flat path. Meanwhile, the energy level in the ground state rapidly increased and approached the $T_{PP}(^3\pi\pi^*)$ state, resulting in the singlet−triplet crossing of $STC(T_{PP}/S_0)$ that was verified to have a diradical configuration distributing the unpaired electrons around the C3 and C7 atoms. The existence of $STC(T_{PP}/S_0)$ facilitated the occurrence of spin inversion of the diradical with high efficiency, thus giving rise to an excellent precursor for the subsequent cyclization reaction. The C3−C7 distance underwent further shortening from ca. 2.8 Å in $STC(T_{PP}/S_0)$ to ca. 1.6 Å in the final product through an ultrafast combination of the diradical toward the major product of **4** in the ground state. However, a sizable barrier (11.9 kcal/mol) was found in the reaction path of the $T_{PP}(^3\pi\pi^*)$ state for **2**−**1** due to the presence of steric hindrance of catalyst **1** (see section 4 of the SI for MEP) when the PCA reaction occurred in the opposite direction, producing the minor product of **5**, which is the enantiomer of **4**. As an important consequence, a high enantioselectivity was achieved for the PCA reaction. Overall, the catalyzed cycloaddition reaction of coumarin is characterized by a barrierless path in the triplet manifold, which has been determined by the DFT/IRC and CASPT2//IRC/CASSCF (12e/10o) computations. The final cyclization takes place in the ground state along a downhill path, which substantially differs the PCA reaction for free coumarin **2** in the singlet hypersurface by overcoming ca. 5.0 kcal/mol barrier (see Scheme 2). This explains why the reaction rate for the **2**−**1**

DOI: 10.1021/acs.joc.6b00980
J. Org. Chem. 2016, 81, 7093−7101

complex in the presence of a chiral Lewis acid is faster than that of isolated **2** in the absence of the Lewis acid besides the alternation in mechanistic course from the triplet to singlet hypersurface.

CONCLUSION

In this work, extensive investigations have been performed by employing state-of-the-art electronic structure calculations to provide the mechanistic comparison regarding how the Lewis acid regulates an enantioselective intramolecular [2 + 2] PCA reaction by using two different substrates. The racemic background reaction of the isolated coumarin is codetermined by a pair of bright $\pi\pi^*$ states through a fast PCA process in the singlet hypersurface and the closure of the reaction channel in a triplet manifold due to an ineffective ISC of $^1\pi\pi^* \rightarrow {}^3\pi\pi^*$, whereas an energetically accessible $^1n\pi^*$ state takes over the PCA reaction of enone substrate **3**, which provides an effective triplet access via an El Sayed type singlet−triplet crossing. For the catalyzed reaction mediated by the boron-based catalysts, the opening of the reaction channel in the triplet state is first beneficial from the accelerated relaxation in the bright $^1\pi\pi^*$ state with a noticeable decrease in the energy of the singly excited state in the presence of an electron-donating (i.e., phenyl ring) and/or -withdrawing (i.e., carbonyl) group. The PCA yield of triplet state is repeatedly verified to be dramatically improved through an enhanced spin−orbit coupling caused by relativistic effects due to heavy atoms in the chiral Lewis acid catalyst. These mechanistic insights together with the previous computational efforts[51] lay the foundation for further studies of PCA reactions mediated by Lewis acid and may help develop a mechanism-based design of enantioselective catalysts.

ASSOCIATED CONTENT

Supporting Information

The Supporting Information is available free of charge on the ACS Publications website at DOI: 10.1021/acs.joc.6b00980.

Computational details, figures, tables and Cartesian coordinates (PDF)

AUTHOR INFORMATION

Corresponding Author

*E-mail: xuebochen@bnu.edu.cn.

Notes

The authors declare no competing financial interest.

ACKNOWLEDGMENTS

Financial support for this work was provided by the NSFC (21373029).

REFERENCES

(1) Ciamician, G.; Silber, P. *Ber. Dtsch. Chem. Ges.* **1908**, *41*, 1928−1935.
(2) Belluš, D.; Ernst, B. *Angew. Chem., Int. Ed. Engl.* **1988**, *27*, 797−827.
(3) Alcaide, B.; Almendros, P.; Aragoncillo, C. *Chem. Soc. Rev.* **2010**, *39*, 783−816.
(4) Lee-Ruff, E.; Mladenova, G. *Chem. Rev.* **2003**, *103*, 1449−1483.
(5) Namyslo, J. C.; Kaufmann, D. E. *Chem. Rev.* **2003**, *103*, 1485−1537.
(6) Poplata, S.; Tröster, S.; Zou, Y. Q.; Bach, T. *Chem. Rev.* **2016**, DOI: 10.1021/acs.chemrev.5b00723.
(7) Ischay, M. A.; Anzovino, M. E.; Du, J.; Yoon, T. P. *J. Am. Chem. Soc.* **2008**, *130*, 12886−12887.
(8) Brimioulle, R.; Bach, T. *Angew. Chem., Int. Ed.* **2014**, *53*, 12921−12924.
(9) Hoffmann, R.; Woodward, R. B. *J. Am. Chem. Soc.* **1965**, *87*, 2046−2048.
(10) Woodward, R. B.; Hoffmann, R. *Angew. Chem., Int. Ed. Engl.* **1969**, *8*, 781−853.
(11) Ciamician, G. *Science* **1912**, *36*, 385−394.
(12) Seiser, T.; Saget, T.; Tran, D. N.; Cramer, N. *Angew. Chem., Int. Ed.* **2011**, *50*, 7740−7752.
(13) Talavera, G.; Reyes, E.; Vicario, J. L.; Carrillo, L. *Angew. Chem., Int. Ed.* **2012**, *51*, 4104−4107.
(14) Suarez-Pantiga, S.; Hernandez-Diaz, C.; Rubio, E.; Gonzalez, J. M. *Angew. Chem.* **2012**, *124*, 11720−11723.
(15) de Nanteuil, F.; Waser, J. *Angew. Chem.* **2013**, *125*, 9179−9183.
(16) Brimioulle, R.; Lenhart, D.; Maturi, M. M.; Bach, T. *Angew. Chem., Int. Ed.* **2015**, *54*, 3872−3890.
(17) Tolbert, L. M.; Ali, M. B. *J. Am. Chem. Soc.* **1982**, *104*, 1742−1744.
(18) Demuth, M.; Palomer, A.; Sluma, H.-D.; Dey, A. K.; Krüger, C.; Tsay, Y.-H. *Angew. Chem., Int. Ed. Engl.* **1986**, *25*, 1117−1119.
(19) Meyers, A. I.; Fleming, S. A. *J. Am. Chem. Soc.* **1986**, *108*, 306−307.
(20) Lu, R.; Yang, C.; Cao, Y.; Wang, Z.; Wada, T.; Jiao, W.; Mori, T.; Inoue, Y. *Chem. Commun.* **2008**, *3*, 374−376.
(21) Inoue, Y.; Wada, T.; Sugahara, N.; Yamamoto, K.; Kimura, K.; Tong, L.-H.; Gao, X.-M; Hou, Z.-J.; Liu, Y. *J. Org. Chem.* **2000**, *65*, 8041−8050.
(22) Fukuhara, G.; Mori, T.; Wada, T.; Inoue, Y. *J. Org. Chem.* **2006**, *71*, 8233−8243.
(23) Lu, R.; Yang, C.; Cao, Y.; Tong, L.; Jiao, W.; Wada, T.; Wang, Z.; Mori, T.; Inoue, Y. *J. Org. Chem.* **2008**, *73*, 7695−7701.
(24) Austin, K. A. B.; Herdtweck, E.; Bach, T. *Angew. Chem., Int. Ed.* **2011**, *50*, 8416−8419.
(25) Müller, C.; Maturi, M. M.; Bauer, A.; Cuquerella, M. C.; Miranda, M. A.; Bach, T. *J. Am. Chem. Soc.* **2011**, *133*, 16689−16697.
(26) Maturi, M. M.; Wenninger, M.; Alonso, R.; Bauer, A.; Pöthig, A.; Riedle, E.; Bach, T. *Chem. - Eur. J.* **2013**, *19*, 7461−7472.
(27) Coote, S. C.; Bach, T. *J. Am. Chem. Soc.* **2013**, *135*, 14948−14951.
(28) Mayr, F.; Wiegand, C.; Bach, T. *Chem. Commun.* **2014**, *50*, 3353−3355.
(29) Alonso, R.; Bach, T. *Angew. Chem., Int. Ed.* **2014**, *53*, 4368−4371.
(30) Lewis, F. D.; Barancyk, S. V. *J. Am. Chem. Soc.* **1989**, *111*, 8653−8661.
(31) Lewis, F. D.; Reddy, G. D.; Elbert, J. E.; Till-berg, B. E.; Meltzer, J. A.; Kojima, M. *J. Org. Chem.* **1991**, *56*, 5311−5318.
(32) Ryu, D. H.; Zhou, G.; Corey, E. J. *J. Am. Chem. Soc.* **2004**, *126*, 4800−4802.
(33) Liu, D.; Canales, E.; Corey, E. J. *J. Am. Chem. Soc.* **2007**, *129*, 1498−1499.
(34) Canales, E.; Corey, E. J. *J. Am. Chem. Soc.* **2007**, *129*, 12686−12687.
(35) Corey, E. J. *Angew. Chem., Int. Ed.* **2009**, *48*, 2100−2117.
(36) Brimioulle, R.; Guo, H.; Bach, T. *Chem. - Eur. J.* **2012**, *18*, 7552−7560.
(37) Guo, H.; Herdtweck, E.; Bach, T. *Angew. Chem., Int. Ed.* **2010**, *49*, 7782−7785.
(38) Brimioulle, R.; Bach, T. *Science* **2013**, *342*, 840−843.
(39) Brimioulle, R.; Bauer, A.; Bach, T. *J. Am. Chem. Soc.* **2015**, *137*, 5170−5176.
(40) Du, J.; Yoon, T. P. *J. Am. Chem. Soc.* **2009**, *131*, 14604−14605.
(41) Ischay, M. A.; Lu, Z.; Yoon, T. P. *J. Am. Chem. Soc.* **2010**, *132*, 8572−8574.
(42) Du, J.; Skubi, K. L.; Schultz, D. M.; Yoon, T. P. *Science* **2014**, *344*, 392−396.
(43) Yoon, T. P.; Ischay, M. A.; Du, J. *Nat. Chem.* **2010**, *2*, 527−532.

DOI: 10.1021/acs.joc.6b00980
J. Org. Chem. 2016, 81, 7093−7101

(44) Lu, Z.; Yoon, T. P. *Angew. Chem., Int. Ed.* **2012**, *51*, 10329−10332.
(45) Ischay, M. A.; Ament, M. S.; Yoon, T. P. *Chem. Sci.* **2012**, *3*, 2807−2811.
(46) Hurtley, A. E.; Lu, Z.; Yoon, T. P. *Angew. Chem., Int. Ed.* **2014**, *53*, 8991−994.
(47) Pham, P. V.; Nagib, D. A.; MacMillan, D. W. C. *Angew. Chem., Int. Ed.* **2011**, *50*, 6119−6122.
(48) Nagib, D. A.; MacMillan, D. W. C. *Nature* **2011**, *480*, 224−228.
(49) McNally, A.; Prier, C. K.; MacMillan, D. W. C. *Science* **2011**, *334*, 1114−1117.
(50) Prier, C. K.; Rankic, D. A.; MacMillan, D. W. C. *Chem. Rev.* **2013**, *113*, 5322−5363.
(51) Wang, H. J.; Cao, X. Y.; Chen, X. B.; Fang, W. H.; Dolg, M. *Angew. Chem., Int. Ed.* **2015**, *54*, 14295−14298.
(52) Bergner, A.; Dolg, M.; Küchle, W.; Stoll, H.; Preuss, H. *Mol. Phys.* **1993**, *80*, 1431−1441.
(53) Dolg, M.; Cao, X. *Chem. Rev.* **2012**, *112*, 403−480.
(54) Su, H. Z.; Chen, X. B.; Fang, W. H. *Anal. Chem.* **2014**, *86*, 891−899.
(55) Han, J.; Chen, X. B.; Shen, L.; Chen, Y.; Fang, W. H.; Wang, H. B. *Chem. - Eur. J.* **2011**, *17*, 13971−1397.
(56) Cui, G. L.; Cao, X. Y.; Fang, W. H.; Dolg, M.; Thiel, W. *Angew. Chem., Int. Ed.* **2013**, *52*, 10281−10285.
(57) Srnec, M.; Chalupský, J.; Fojta, M.; Zendlová, L.; Havran, L.; Hocek, M.; Kývala, M.; Rulíšek, L. *J. Am. Chem. Soc.* **2008**, *130*, 10947−10954.
(58) Fukui, K. *Acc. Chem. Res.* **1981**, *14*, 363−368.
(59) Hratchian, H. P.; Schlegel, H. B. *J. Chem. Phys.* **2004**, *120*, 9918−9924.
(60) Karlström, G.; Lindh, R.; Malmqvist, P.- Å.; Roos, B. O.; Ryde, U.; Veryazov, V.; Widmark, P.-O.; Cossi, M.; Schimmelpfennig, B.; Neogrady, P.; Seijo, L. *Comput. Mater. Sci.* **2003**, *28*, 222−239.
(61) Werner, H. J.; Knowles, P. J. *J. Chem. Phys.* **1985**, *82*, 5053−5063.
(62) Andersson, K.; Malmqvist, P. Å.; Roos, B. O.; Sadlej, A. J.; Wolinski, K. *J. Phys. Chem.* **1990**, *94*, 5483−5488.
(63) Andersson, K.; Malmqvist, P. Å.; Roos, B. O. *J. Chem. Phys.* **1992**, *96*, 1218−1226.
(64) Frisch, M. J.; Trucks, G. W.; Schlegel, H. B.; Scuseria, G. E.; Robb, M. A.; Cheeseman, J. R.; Montgomery, J. A., Jr.; Vreven, T.; Kudin, K. N.; Burant, J. C.; Millam, J. M.; Iyengar, S. S.; Tomasi, J.; Barone, V.; Mennucci, B.; Cossi, M.; Scalmani, G.; Rega, N.; Petersson, G. A.; Nakatsuji, H.; Hada, M.; Ehara, M.; Toyota, K.; Fukuda, R.; Hasegawa, J.; Ishida, M.; Nakajima, T.; Honda, Y.; Kitao, O.; Nakai, H.; Klene, M.; Li, X.; Knox, J. E.; Hratchian, H. P.; Cross, J. B.; Adamo, C.; Jaramillo, J.; Gomperts, R.; Stratmann, R. E.; Yazyev, O.; Austin, A. J.; Cammi, R.; Pomelli, C.; Ochterski, J. W.; Ayala, P. Y.; Morokuma, K.; Voth, G. A.; Salvador, P.; Dannenberg, J. J.; Zakrzewski, V. G.; Dapprich, S.; Daniels, A. D.; Strain, M. C.; Farkas, O.; Malick, D. K.; Rabuck, A. D.; Raghavachari, K.; Foresman, J. B.; Ortiz, J. V.; Cui, Q.; Baboul, A. G.; Clifford, S.; Cioslowski, J.; Stefanov, B. B.; Liu, G.; Liashenko, A.; Piskorz, P.; Komaromi, I.; Martin, R. L.; Fox, D. J.; Keith, T.; Al-Laham, M. A.; Peng, C. Y.; Nanayakkara, A.; Challacombe, M.; Gill, P. M. W.; Johnson, B.; Chen, W.; Wong, M. W.; González, C.; Pople, J. A. *Gaussian03*, Revision C.02; Gaussian, Inc.: Pittsburgh, PA, 2004.
(65) El-Sayed, M. A. *Acc. Chem. Res.* **1968**, *1*, 8−16.
(66) El-Sayed, M. A. *J. Chem. Phys.* **1963**, *38*, 2834.
(67) Shaik, S. S. *J. Am. Chem. Soc.* **1979**, *101*, 2736−2738.
(68) Shaik, S. S.; Epiotis, N. D. *J. Am. Chem. Soc.* **1980**, *102*, 122−131.

DOI: 10.1021/acs.joc.6b00980
J. Org. Chem. 2016, 81, 7093−7101